Supplement of Atmos. Chem. Phys., 20, 15811–15833, 2020
https://doi.org/10.5194/acp-20-15811-2020-supplement

Atmospheric Chemistry and Physics
Open Access
EGU

Supplement of

Chemical composition and source apportionment of atmospheric aerosols on the Namibian coast

Danitza Klopper et al.

Correspondence to: Paola Formenti (paola.formenti@lisa.ipsl.fr)

Table S1. Correction factor used to scale up the elemental concentrations measured by XRF to account for the X-ray self-attenuation effects in the individual particle grains. A mean diameter of 4.5 μm is chosen to represent the average coarse particle size.

	Na	Mg	Al	Si	P	S	Cl	K	Ca
Correction factor	0.53	0.67	0.77	0.76	0.88	0.9	0.9	0.91	1

Table S2. List of mineral dust episodes identified by peaks in Al and nssCa^{2+} above background concentrations. The start and end dates and times of measurements are provided in UTC.

Episode identifier	Start and end date (UTC)
Dust_2016_01	28/02/2016 04h – 01/03/2016 16h
Dust_2016_02	21/03/2016 07h – 23/03/2016 16h
Dust_2016_03	05/04/2016 20h – 09/04/2016 05h
Dust_2016_04	23/07/2016 08h – 25/07/2016 17h
Dust_2016_05	27/08/2016 20h – 30/08/2016 05h
Dust_2016_06	16/09/2016 19h – 19/09/2016 16h
Dust_2016_07	07/10/2016 07h – 10/10/2016 16h
Dust_2017_01	25/02/2017 19h – 27/02/2017 04h
Dust_2017_02	25/03/2017 19h – 27/03/2017 16h
Dust_2017_03	29/03/2017 19h – 01/04/2017 16h
Dust_2017_04	19/05/2017 08h – 20/05/2017 17h
Dust_2017_05	24/05/2017 20h – 26/05/2017 05h
Dust_2017_06	11/07/2017 08h – 13/07/2017 05h
Dust_2017_07	04/08/2017 20h – 06/08/2017 05h
Dust_2017_08	03/09/2017 09h – 05/09/2017 18h
Dust_2017_09	23/09/2017 21h – 24/09/2017 18h
Dust_2017_10	05/10/2017 21h – 08/10/2017 06h
Dust_2017_11	15/11/2017 09h – 18/11/2017 06h
Dust_2017_12	30/11/2017 09h – 01/12/2017 18h
Dust_2017_13	15/12/2017 09h – 19/12/2017 06h

Figure S1. Scatterplots of Cl, Mg, K, Ca, Na and MSA+SO_4^{2-}/S mass ratios obtained by ion chromatography and XRF analysis showing the slope and distribution of data as well as the Pearson correlation coefficient (R^2).

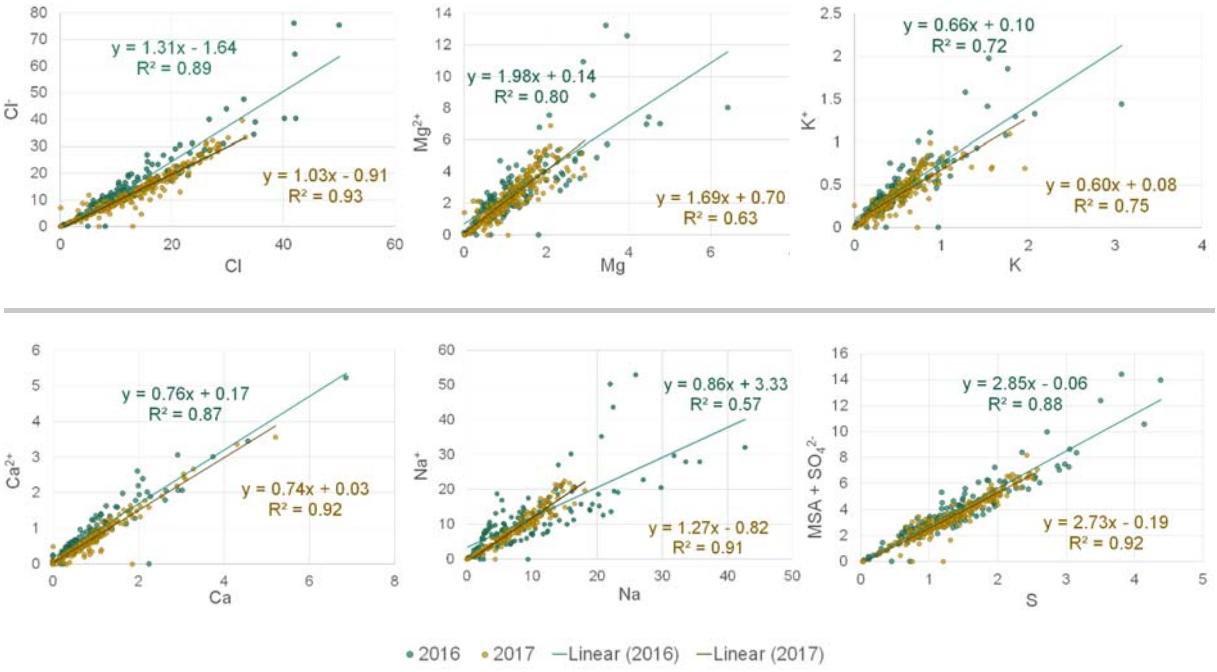

Figure S2. Gridded frequency plot of the variability of the 72-h air mass back-trajectories run for sampling periods in 2016 and 2017 (except the long-range transported air masses in September 2016 and November 2017, which show air masses arriving from as far south as 74°S) run for 21 of the 26 filter sampling periods. Back-trajectories were initiated at 250 m agl. The grid colour indicates the percentage of trajectories of the total trajectories run for all sampling periods, passing the over the 1° x 1° grid.

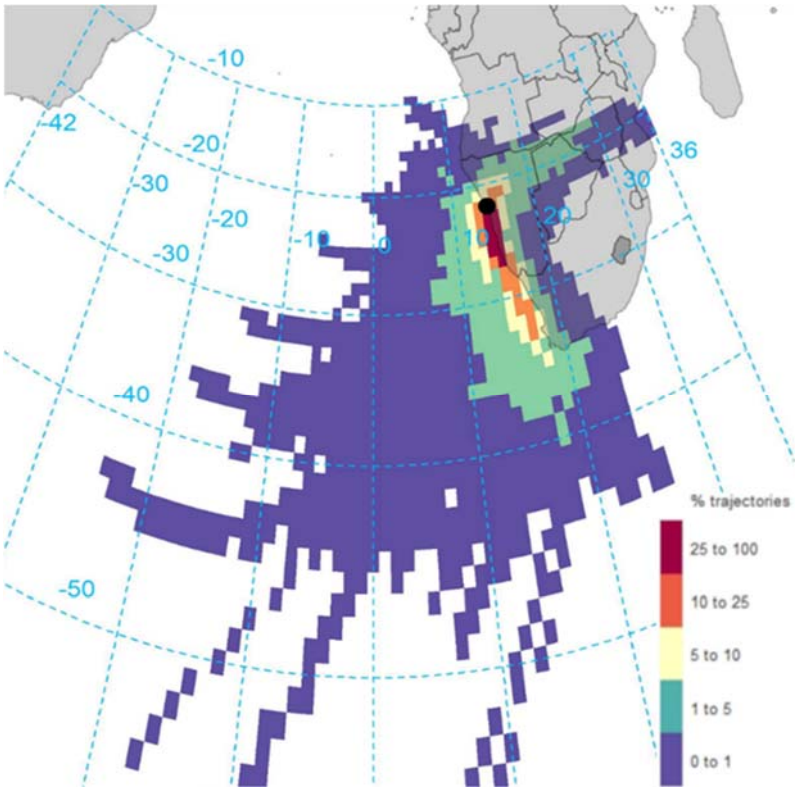

Figure S3. PMF mass apportionment for the five component solution.

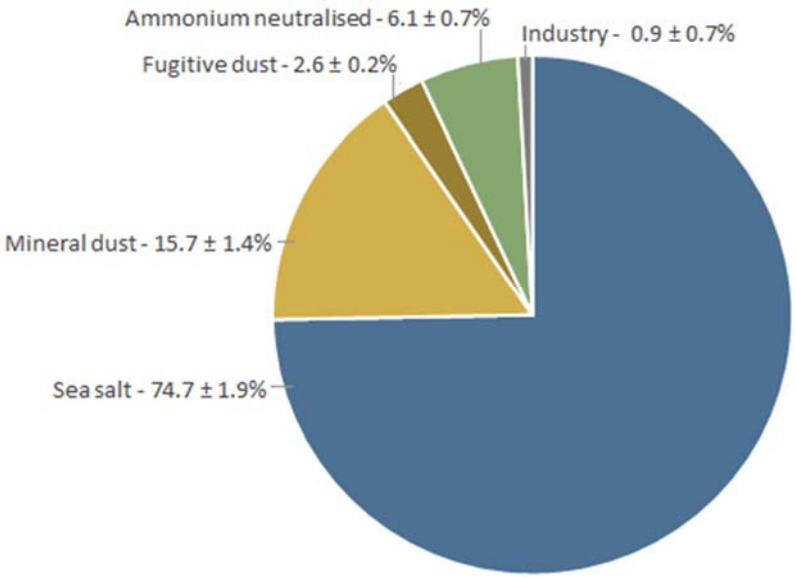

Figure S4. Bivariate polar plots for (a) vanadium and (b) nickel, showing the variability in mean concentrations with changes in wind speed and direction. Wind direction is indicated by the cardinal point in the four quadrants, mean wind speed (m s^{-1}) is indicated by the concentric circles from the centre of the plot and the mean concentrations are measured in ng m^{-3}, and given by the gradient colour scale.

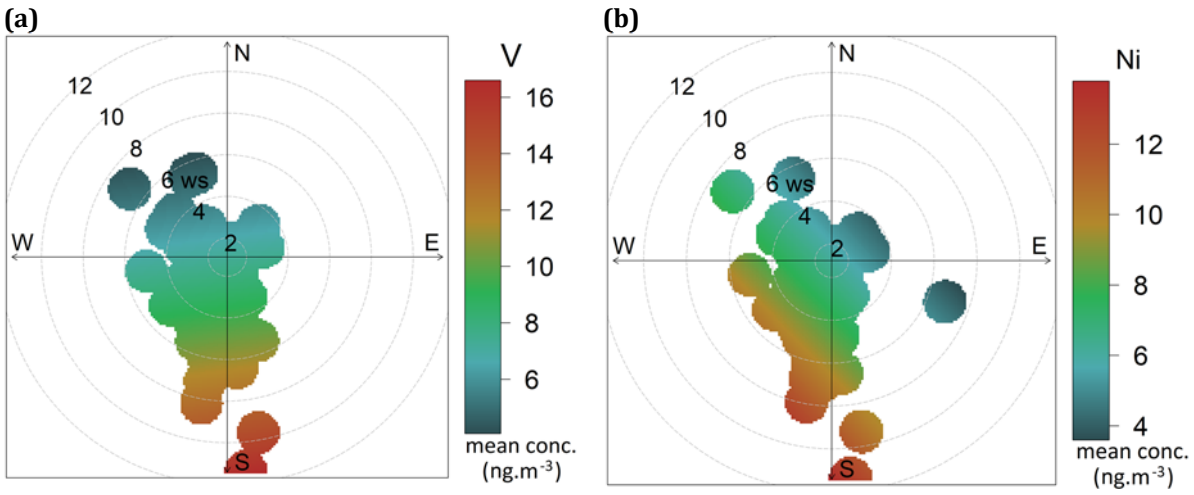

Figure S5. Pie charts of the PMF mass apportionment of V and Ni measured at HBAO. Legends provide with the name of the source component and the fraction of the contributed mass elemental concentration.

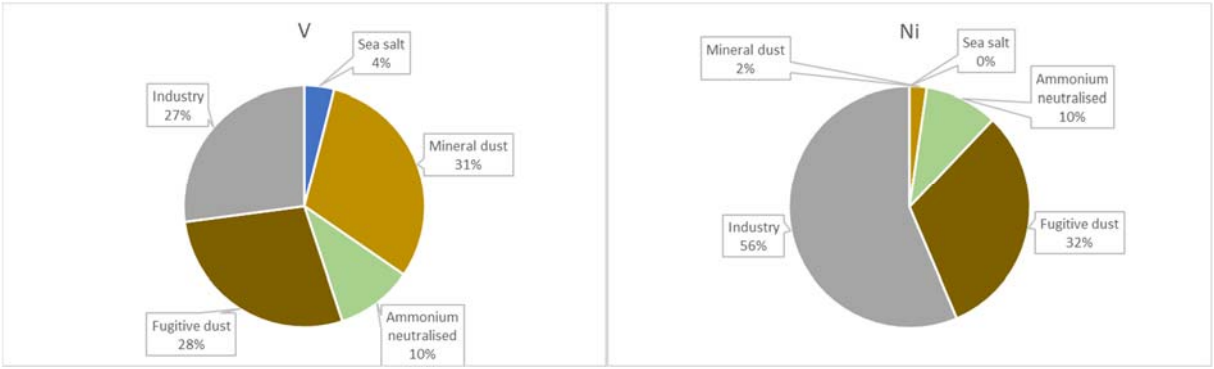

Figure S6. Scatterplot of F^- with respect to $nssCa^{2+}$ for 2016 (blue) and 2017 (orange). Concentrations are expressed in μg m^{-3}. The slope and the Pearson correlation coefficient (R^2) are indicated.

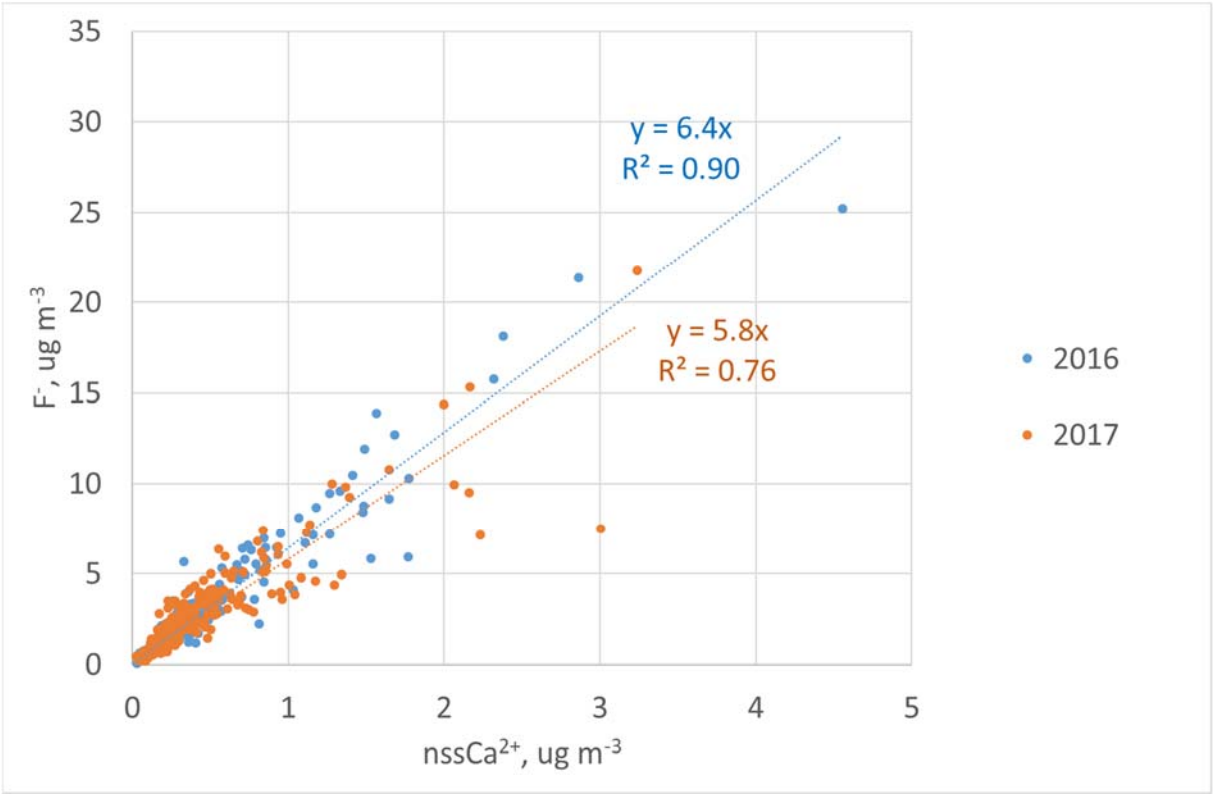

Figure S7. Same as Figure S5 for F^- concentrations.